give η^3 species, but further slippage to η^1 species has not been reported. However, it is important to note that in the absence of 2e-donor ligands the rate of thermal conversion of $(\eta^3$-$C_5Cl_5)Mn(CO)_4$ to $(\eta^5$-$C_5Cl_5)Mn(CO)_3$ at 220 K is 10^4 times slower than the extrapolated rate for the conversion of $(\eta^5$-$C_5H_5)(\eta^3$-$C_5H_5)Fe(CO)$ to $(\eta^5$-$C_5H_5)_2Fe$.[19] This decrease in the thermal ring slippage rate is presumably due to the electron-withdrawing effect of the Cl substituents on the cyclopentadienyl ring, which slows the coordination from that found in the C_5H_5 case. The importance of $\eta^3 \rightarrow \eta^1$-$C_5H_5$ conversion versus the $\eta^3 \rightarrow \eta^5$-$C_5H_5$ process requires experimental investigation.

Acknowledgment. We thank the National Science Foundation for support of this research. In addition, K.M.Y. is grateful to the Natural Sciences and Engineering Research Council of Canada for support as a graduate fellow, 1985-1989.

Registry No. $(\eta^1$-$C_5Cl_5)Mn(CO)_5$, 53158-67-1; $(\eta^3$-$C_5Cl_5)Mn(CO)_4$, 123001-82-1; $(\eta^5$-$C_5Cl_5)Mn(CO)_3$, 56282-21-4; *cis*-$(\eta^1$-$C_5Cl_5)Mn(CO)_4PPh_3$, 122967-78-6; $Mn(CO)_5Cl$, 14100-30-2; $Mn(CO)_5Br$, 14516-54-2; $Mn(CO)_5I$, 14879-42-6; $Mn_2(CO)_{10}$, 10170-69-1; $[Mn(CO)_4Cl]_2$, 18535-43-8; $(\eta^1$-$C_6H_5CH_2)Mn(CO)_5$, 14049-86-6; $(\eta^3$-$C_6H_5CH_2)Mn(CO)_4$, 122967-79-7; *cis*-$(\eta^1$-$C_6H_5CH_2)Mn(CO_4)PPh_3$, 54834-89-8; $C_{10}Cl_{10}$, 2227-17-0; $C_{10}Cl_8$, 6298-65-3; C_5Cl_6, 77-47-4; $(C_6H_5CH_2)_2$, 103-29-7; $(\eta^5$-$C_5Cl_5)Mn(CO)_2$, 119272-39-8; $[(\eta^5$-$C_5H_5)Fe(CO)_2]_2$, 12154-95-9; $(\eta^5$-$C_5H_5)Fe(CO)_2Cl$, 12107-04-9.

(38) Kowaleski, R. M.; Rheingold, A. L.; Trogler, W. C.; Basolo, F. *J. Am. Chem. Soc.* **1986**, *108*, 2460.
(39) Pope, K. R.; Wrighton, M. S. *J. Am. Chem. Soc.* **1987**, *109*, 4545.

Synthesis and Characterization of a Paramagnetic Osmium-Ruthenium Double Bond

James P. Collman* and James M. Garner

Contribution from the Chemistry Department, Stanford University, Stanford, California 94305.
Received January 6, 1989

Abstract: Using a cofacial biphenylene-bridged bis(porphyrin) (DPB, 1,8-bis[5-(2,8,13,17-tetraethyl-3,7,12,18-tetramethyl)porphyrin]biphenylene), a general synthetic method for the preparation of heterodinuclear complexes with 3d, 4d, and 5d transition metals is described. For $(Os^{II})(Ru^{II})$DPB, and DPB ligand provides a high local concentration of the mixed-metal pair, thereby controlling the stoichiometry of the metal-metal interaction and facilitating the formation of an intramolecular, paramagnetic, osmium-ruthenium double bond. The magnetic and spectroscopic properties are found to be similar to those of the analogous homodinuclear ruthenium and osmium DPB compounds.

Heteronuclear metal-metal multiple bonds in complexes with $L_4MM'L_4$ structures remain a curiosity within this subfield of inorganic chemistry. The molecular orbital diagram,[1] which correctly predicts many of the physical properties of homonuclear dimers with this structure, can be used to predict that numerous heteronuclear combinations of transition metal should also form the same types of metal-metal multiple bonds (Figure 1).[2] However, few of these compounds have yet to be prepared and characterized.[3] The problem is likely not the intrinsic thermodynamic instability of such heteronuclear metal-metal bonds relative to their homonuclear counterparts but, rather, the lack of convergent synthetic methods for their preparation and isolation. Problems associated with indirect methods for the preparation of heteronuclear metal-metal bonds can be illustrated by the reaction in eq 1. Vacuum pyrolysis of an intimate mixture of

$$Ru(OEP)(Py)_2 + Os(OEP)(Py)_2 \rightarrow [Ru(OEP)]_2 + [(OEP)RuOs(OEP)] + [Os(OEP)]_2 \quad (1)$$

mononuclear Ru and Os porphyrin bis(pyridine) complexes yields a nonstoichiometric mixture of three products as determined by ^1H NMR.[4] Two of these products are identified as the homonuclear Ru and Os porphyrin dimers, and the new complex is postulated as the heteronuclear dimer containing a paramagnetic Os=Ru bond. Attempts to isolate the heteronuclear dimer in order to study its magnetic, spectroscopic, and chemical properties are difficult due to the similarity in physical properties (solubility, instability on chromatographic supports, etc.) to the mononuclear dimers. Hence, difficulties in controlling stoichiometry and isolating the heteronuclear product from other reaction products frustrate the synthesis of these interesting compounds.

Our approach to solving this problem originates from another research project within our group concerning the development of molecular catalysts for the reduction of dioxygen via the four-electron pathway. Most of the successful catalysts for this reaction utilize a cofacial bis(porphyrin) ligand, which allows two 3d metals to be held in close proximity such that both can act cooperatively in the reduction of an axially bound dioxygen molecule.[5] For 4d and 5d transition metals, it seemed likely that such ligands allow a sufficiently close approach of the two metals that strong metal-metal bonding interactions would occur in the absence of axial ligands. We have since demonstrated this with the synthesis and characterization of the homonuclear compounds, $(Ru^{II})_2$DPB and $(Mo^{II})_2$DPB (DPB represents a biphenylene-bridged cofacial bis(porphyrin); Figure 2). The presence of intramolecular metal-metal bonds in these compounds is based upon magnetic susceptibility, ^1H NMR, and UV-visible similarities to the analogous OEP dimers.[6]

(1) Cotton, F. A.; Curtis, N. F.; Harris, C. B.; Johnson, B. F. G.; Lippard, S. J.; Mague, J. T. *Robinson*, W. R.; Wood, J. S. *Science* **1964**, *145*, 1305.
(2) As pointed out to us by Prof. Cotton, the spin states of some of the heteronuclear compounds tabulated in this figure may differ from these predicted values. For example, he and others have shown that the δ^* and π^* metal-metal orbitals for the mixed-valence compound, $Ru_2(O_2CC_3H_7)_4Cl$, are close in energy, leading to a quartet instead of a doublet spin state. However, all of the present data for the homonuclear porphyrin dimers is consistent with metal-metal orbitals, which are well separated in energy [i.e., $[Ru(OEP)]_2^+(BF_4^-)$ is low spin, $\mu_{eff} = 1.8 \pm 0.3\ \mu_B$). We must therefore wait for the compounds to be prepared to see whether the spin-state predictions hold true.
(3) Morris, R. H. *Polyhedron* **1987**, *6*, 793. This paper gives a review of quadruply bonded, chromium triad heterodinuclear complexes.
(4) Barnes, C. E. Ph.D. Thesis, Stanford University, 1982. Woo, L. K. Ph.D Thesis, Stanford University, 1984.
(5) (a) Collman, J. P.; Hendricks, N. H.; Leidner, C. R.; Ngameni, E.; L'Her, M. *Inorg. Chem.* **1988**, *27*, 387, and references therein. (b) Ni, C.; Abdalmuhdi, I.; Chang, C. K.; Anson, F. C. *J. Chem.* **1987**, *91*, 1158.
(6) Collman, J. P.; Kim, K.; Garner, J. M. *J. Chem. Soc., Chem. Commun.* **1986**, 1711.

0002-7863/90/1512-166$02.50/0

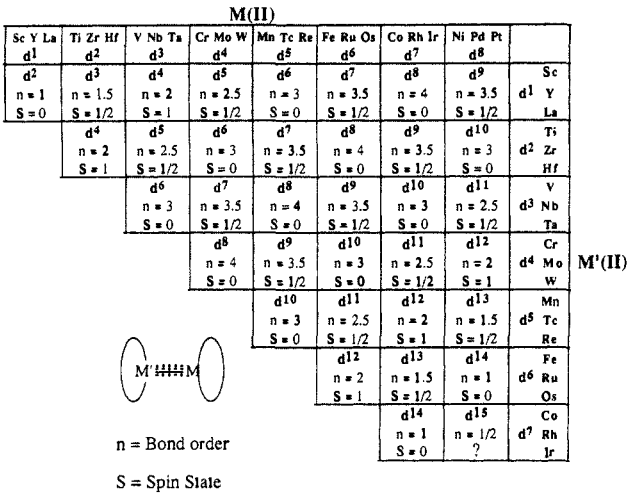

Figure 1. Possible transition-metal combinations for neutral metalloporphyrin dimers containing heteronuclear metal–metal bonds.

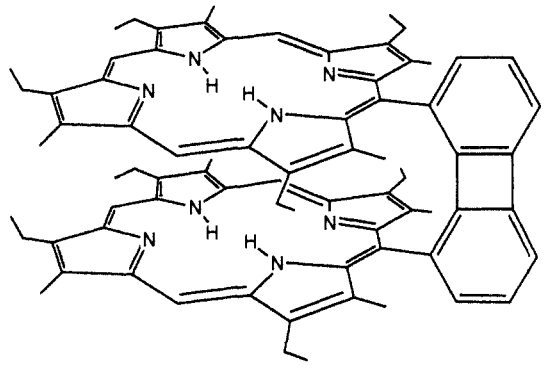

Figure 2. Structure of the biphenylene-bridged cofacial bis(porphyrin), H_4DPB.

The cofacial diporphyrin ligand alleviates many of the indirect synthetic problems mentioned above. The stoichiometry can be controlled by providing a high local concentration of the mixed-metal pair, thus facilitating the formation of the intramolecular heteronuclear metal–metal bond. Intermolecular homonuclear metal–metal bonding may be sufficiently disfavored that such products will not be formed in any significant amount, thus allowing the isolation and purification of the heteronuclear product. Herein, we report the application of this approach to the synthesis and characterization of a cofacial bis(porphyrin) complex with a paramagnetic osmium–ruthenium double bond.

Experimental Section

Solvents and Reagents. All solvents for glovebox use were distilled from their blue or purple sodium benzophenone ketyl solutions (toluene, benzene, THF, and cyclohexane), from KOH and then BaO (pyridine), from P_2O_5 (CH_2Cl_2), or from $NaOCH_3$ (CH_3OH) under a dry nitrogen atmosphere. These solvents were subsequently degassed in the glovebox by bubbling box-atmosphere gas through the solvent for 20–30 min. Deuterated solvents ($C_6D_5CD_3$, C_6D_6) for oxygen-sensitive complexes were dried similarly and then degassed on a vacuum line (10^{-5} Torr) with three successive freeze–pump–thaw cycles and stored in the glovebox. $CDCl_3$ for routine spectra was passed down a basic alumina column prior to use. Flash chromatographic silica (EM Science, Kieselgel 60H), gravity alumina (Fisher, Neutral, 80–200 mesh), and Celite for glovebox use were predried at 300 °C overnight and then further dried and degassed under vacuum (300 °C, 10^{-2} Torr) for 24 h and stored in the glovebox. All other reagents were used as received. H_4DPB was prepared by a modification of the literature procedure.[7]

Instruments and Measurements. UV photochemical experiments utilized a Canrad-Hanovia 450-W medium-pressure mercury immersion lamp with Ace Glass 100-mL borosilicate or 500-mL quartz, water-cooled reaction vessels. Manipulations of air-sensitive compounds were performed either in a glovebox, in Schlenkware, or on a vacuum line. The glovebox was a Vacuum/Atmospheres HE-553-2 Dri-Lab with a MO-40-1H Dri-Train under nitrogen atmosphere ($O_2 \leq 1$ ppm). Oxygen levels were monitored with a AO 316-C trace oxygen analyzer. ^1H NMR spectra were recorded with a 300-MHz Nicolet NMC-300 instrument with a FT 1280 disk data system, and all chemical shifts are reported relative to tetramethylsilane. Variable-temperature experiments with this instrument were calibrated by the frequency difference method[8] with neat methanol (≤30 °C) or ethylene glycol (>30 °C) solutions in separate NMR tubes. A Cary 219 spectrophotometer was used to record UV–visible spectra (300–825 nm), and infrared spectra were obtained with KBr pellet samples using an IBM 98 FT-IR instrument. LSI and FAB mass spectroscopy used tetraglyme and sulfolane liquid matrixes, respectively, and calculated isotope intensities matched well with the observed molecular or fragment ion isotope clusters for all mass spectra. Solution magnetic susceptibility measurements (21 °C) utilized the Evans method[9a] with Wilmad precision coaxial NMR tubes and are corrected for ligand diamagnetism with the literature value for a porphyrin[9b] and Pascal's constants[9c] for the substituents.

(Zn)(H_2)DPB (1). With a syringe pump, $Zn(O_2CCH_3)_2{\cdot}2H_2O$ (179 mg, 0.814 mmol) dissolved in CH_3OH (10 mL) was added (0.0144 mL/min) to a refluxing CH_2Cl_2 solution (1600 mL) of H_4DPB (1.000 g, 0.905 mmol). The resulting solution was evaporated, redissolved in CH_2Cl_2, and then flash chromatographed (SiO_2, 2 × 12 cm). A bright red band of $(Zn)_2DPB$ eluted with CH_2Cl_2. A 2–4% methanolic CH_2Cl_2 solution eluted the brown-red product band. This band was evaporated and crystallized from CH_2Cl_2/CH_3OH to yield purple needles, which were washed with CH_3OH and dried under vacuum (721 mg, 76%, based upon $Zn(O_2CCH_3)_2{\cdot}2H_2O$). ^1H NMR (C_6D_6, ppm): H_{meso}, 9.32 (s, 1 H), 8.85 (s, 2 H), 8.81 (s, 1 H), 8.74 (s, 2 H); biphenylene, 7.00 and 6.98 (two overlapping d, 2 H total), 6.89 and 6.84 (overlapping d and t, respectively, 2 H total), 6.59 (t, 7.4 Hz, 1 H), 6.22 (d, 7.5 Hz, 1 H); CH_2CH_3, 4.25–3.50 (m, 16 H); CH_3, 3.28 (s, 6 H), 3.26 (s, 6 H), 3.22 (s, 6 H), 3.05 (s, 6 H); CH_2CH_3, 1.77 (t, 7.4 Hz, 6 H), 1.63 and 1.58 (two overlapping t, 12 H total), 1.42 (t, 7.6 Hz, 6 H); N–H, −7.50 (br s, 1 H) and −7.53 (br s, 1 H). EIMS: *m/e* 1167 (cluster, M^+). UV-vis (CH_2Cl_2/py): λ_{max} (log ε) 386 (5.29), 516 (3.91), 544 (3.98), 578 (3.91), 629 nm (3.22). Anal. Calcd for $C_{76}H_{78}N_8Zn$: C, 78.09; H, 6.73; N, 9.59. Found: C, 78.20; H, 6.76; N, 9.65. The unreacted H_4DPB can be recovered by eluting the column with 5% methanolic CH_2Cl_2.

(Ru)(H_2)DPB(CO)(CH_3OH) (2). Under an argon atmosphere, **1** (50 mg, 0.043 mmol) and $Ru_3(CO)_{12}$ (50 mg, 0.078 mmol) were heated at reflux in 2-methoxyethanol (5 mL) for a total of 7 h. After 2.5 and 5 h, $Ru_3(CO)_{12}$ (25 mg) was added to the reaction solution and heating was continued. The mixture was cooled and poured into a brine solution (30 mL). After stirring (15 min), the red precipitate was collected on a Celite pad and washed with water (100 mL). The Celite pad was washed with CH_2Cl_2, and the red filtrate was evaporated. The residue was flash chromatographed (SiO_2, 2 × 8 cm, toluene), and the first red band was collected and evaporated. (Ru)(Zn)DPB(CO)(OH_2). LSIMS: *m/e* 1297 (cluster, $M^+ - OH_2$), 1268 (cluster $M^+ - OH_2 - CO$). With vigorous stirring, the residue was redissolved in CH_2Cl_2/CH_3OH (2/1, 10 mL total) and treated with 6 M HCl (2 mL) for 15 min. The aqueous phase was made basic with solid Na_2CO_3, and the mixture was again stirred vigorously for 15 min. The organic phase was separated and evaporated. The residue was flash chromatographed (SiO_2, 2 × 18 cm, toluene), and the major brown-red band was collected and crystallized from CH_2Cl_2/CH_3OH at −20 °C to yield a red-purple solid (41 mg, 76%). ^1H NMR ($CDCl_3$, ppm) of major isomer: H_{meso}, 9.10 (s, 2 H), 9.00 (s, 1 H), 8.63 (s, 1 H), 8.51 (s, 2 H); biphenylene, 7.24–7.04 (m); CH_2CH_3, 4.20–3.62 (m); CH_3, 3.50 (s, 6 H), 3.33 (s, 6 H), 3.01 (s, 6 H), 2.92 (s, 6 H); CH_2CH_3, 1.74 and 1.72 (overlapping t, 12 H total), 1.60 and 1.54 (overlapping t, 12 H total); N–H, −10.36 (br s, 2 H). FDMS: *m/e* 1233 (cluster, $M^+ - CH_3OH$). UV-vis (toluene/py): λ_{max} (log ε) 397 (5.39), 506 (4.20), 527 (4.16), 555 (4.09), 570 sh (3.75), 627 nm (3.31). IR: 1927 cm^{-1} (CO). Anal. Calcd for $C_{78}H_{82}N_8O_2Ru$: C, 74.08; H, 6.54; N, 8.86. Found: C, 74.37; H, 6.44; N, 8.95.

(Os)(H_2)DPB(CO)(CH_3OH) (3). Under an argon atmosphere, **1** (50 mg, 0.043 mmol) and $Os_3(CO)_{12}$ (30 mg, 0.033 mmol) were heated at reflux in ethyl digol (6 mL) for 3 h. The porphyrinic product was precipitated and purified exactly as described for the analogous ruthenium complex. (Os)(Zn)DPB(CO)(OH_2). LSIMS: *m/e* 1322 (cluster, $M^+ - OH_2$), 1356 (cluster, $M^+ - OH_2 - CO$). The zinc porphyrin in this

(7) (a) Chang, C. K.; Abdalmuhdi, I. *Angew. Chem., Int. Ed. Engl.* **1984**, *23*, 164. (b) Eaton, S. S.; Eaton, G. R.; Chang, C. K. *J. Am. Chem. Soc.* **1985**, *107*, 3177. (c) Kim, K. Ph.D. Thesis, Stanford University, 1986.

(8) Van Geet, A. N. *Anal. Chem.* **1968**, *40*, 2227.

(9) (a) Baker, M. V.; Field, L. D.; Hambley, T. N. *Inorg. Chem.* **1988**, *16*, 2872. This paper gives the Evans equation for a NMR spectrometer with a superconducting magnet. (b) Eaton, S. S.; Eaton, G. R. *Ibid.* **1980**, *19*, 1095. (c) Jolly, W. L. *The Synthesis and Characterization of Inorganic Compounds*; Prentice-Hall: Englewood Cliffs, NJ, 1970; p 371.

complex was demetalated and purified exactly as described for the ruthenium analogue. The product crystallized as purple blades from CH_2Cl_2/CH_3OH (34 mg, 59%). ^1H NMR ($CDCl_3$, ppm): H_{meso}, 9.13 (s, 2 H), 9.06 (s, 1 H), 8.45 (s, 2 H), 8.37 (s, 1 H); biphenylene, 7.22–7.00 (m, 6 H total); CH_2CH_3, 4.10 (m, 4 H), 3.83 (m, 8 H), 3.66 (m, 4 H); CH_3, 3.54 (s, 6 H), 3.32 (s, 6 H), 2.99 (s, 6 H), 2.90 (s, 6 H); CH_2CH_3, 1.74 and 1.71 (overlapping t, 12 H total), 1.58 and 1.56 (overlapping t, 12 H total); N–H, −10.13 (br s, 2 H). UV–vis (toluene/py): λ_{max} (log ϵ) 395 (5.49), 410 sh (5.07), 505 (4.37), 537 (4.27), 572 (3.85), 626 nm (3.51). LSIMS: *m/e* 1321 (cluster, $M^+ - CH_3OH$), 1294 (cluster, $M^+ - CH_3OH - CO$). IR: 1892 cm^{-1} (CO). Anal. Calcd for $C_{78}H_{82}N_8O_2Os$: C, 69.20; H, 6.11; N, 8.28. Found: C, 68.99; H, 5.98; N, 8.40.

$(Os)_2DPB(CO)_2(Py)_2$ (4). Under an argon atmosphere, H_4DPB (100 mg, 0.0905 mmol) and $Os_3(CO)_{12}$ (83 mg, 0.092 mmol) were heated at reflux in ethyl digol (10 mL) for 3 h. The solution was cooled and then transferred via cannula into a degassed (bubbled with argon for 15 min) aqueous brine solution (25 mL). The red precipitate was filtered through a Celite pad in the air, washed with water (100 mL), and vacuum dried at 25 °C over P_2O_5. The Celite pad was taken into the glovebox for purification and crystallization. The pad was washed with toluene until the filtrate was colorless, and then the red filtrate was concentrated and flash chromatographed (SiO_2, 2 × 18 cm, toluene). The first pink-red band was collected, evaporated, heated at reflux with neat pyridine (15 min), and then crystallized from cyclohexane to yield a red powder (126 mg, 82%). ^1H NMR (C_6D_6, ppm): H_{meso}, 9.69 (s), 9.56 (s), 9.45 (s), 9.35 (s), 9.32 (s), 9.08 (s); biphenylene, 7.32–6.07 (m); CH_2CH_3, 3.80–3.30 (m); CH_3, 3.74 (s), 3.66 (s), 3.54 (s), 2.98 (s), 2.95 (s), 2.88 (s); outer pyridine, H_p 4.68 (t), H_m 3.91 (t), H_o 1.08 (d, 5.1 Hz); inner pyridine, H_p 4.30 (t), H_m 2.61 (t), H_o 0.22 (d); CH_2CH_3, 1.63 (t, 7.4 Hz), 1.62 (t, 7.8 Hz), 1.59 (t, 7.7 Hz), 1.53 (t, 7.5 Hz). LSIMS: *m/e* 1696 (cluster, M^+), 1617 (cluster, M^+ – py), 1538 (cluster, M^+ – 2 py). UV–vis (toluene/py): λ_{max} (log ϵ) 397 (5.51), 515 (4.35), 540 (4.39), 592 sh nm (3.55). IR: 1902 cm^{-1} (CO). Anal. Calcd for $C_{88}H_{86}N_{10}O_2Os_2$: C, 62.32; H, 5.11; N, 8.26. Found: C, 60.92; H, 5.02; N, 7.89.

(Os)(Ru)DPB$(CO)_2(CH_3OH)_2$ (5). Under an argon atmosphere, **2** (30 mg, 0.024 mmol) and $Os_3(CO)_{12}$ (20 mg, 0.022 mmol) were heated at reflux in ethyl digol (5 mL) for 3.5 h. The crude solid was isolated as described for **4** and then purified by flash chromatography (SiO_2, 2 × 18 cm, toluene) in the glovebox. The first red-orange band was collected, evaporated, and crystallized from CH_2Cl_2/CH_3OH as a red-orange solid (26 mg, 72%). ^1H NMR ($CDCl_3$, ppm): H_{meso}, 9.06 (s, 1 H), 8.96 (s, 2 H), 8.91 (s, 1 H), 8.75 (s, 2 H); biphenylene, 7.30–7.18 (m), 7.15–7.00 (m), 6.93 (d, 8.2 Hz, 1 H), 6.86 (d, 8.0 Hz, 1 H); CH_2CH_3, 3.80–3.45 (m, 16 H total); CH_3, 3.23 (s, 6 H), 3.18 (s, 6 H), 3.04 and 3.04 (overlapping s, 12 H total); CH_2CH_3, 1.63 and 1.61 (overlapping t, 12 H), 1.38 and 1.36 (overlapping t, 12 H). LSIMS: *m/e* 1446 (cluster, $M^+ - 2\,CH_3OH$). UV–vis (toluene/py): λ_{max} (log ϵ) 397 (5.35), 524 (4.22), 542 (4.19), 553 nm (4.08). IR: 1931, 1905 sh, 1865 cm^{-1} (CO). Anal. Calcd for $C_{80}H_{84}N_8O_4OsRu$: C, 63.51; H, 5.60; N, 7.41. Found: C, 63.70; H, 5.66; N, 7.49.

(Ru)(H_2)DPB$(Py)_2$ (6). A solution of **2** (40 mg, 0.032 mmol) in pyridine (100 mL) was added to a borosilicate photoreactor and then degassed with argon (20 min). With a slow purge of argon, the solution was irradiated with the mercury lamp for 36 h. During this time, the 552-nm band of the ruthenium carbonyl complex disappeared and was monitored to determine the completion of the reaction. The pyridine solution was evaporated. The residue was taken into the glovebox, dissolved in THF, and chromatographed (Al_2O_3, 0.5 × 5 cm, THF). The brown-orange eluant was evaporated and dried under vacuum (33 mg, 77%). ^1H NMR (C_6D_6, ppm): H_{meso}, 9.78 (s, 2 H), 9.56 (s, 1 H), 9.00 (s, 1 H), 8.91 (s, 2 H); biphenylene, 7.06 (d, 6.0 Hz, 1 H), 6.95 (d, 7.4 Hz, 1 H), 6.79 (t, 7.3 Hz, 1 H), 6.62 (d, 8.5 Hz, 1 H), 6.59 (t, 1 H), 6.24 (d, 7.3 Hz, 1 H); CH_2CH_3, 3.94 (m), 3.84–3.42 (overlapping m); CH_3, 3.61 (s, 6 H), 3.49 (s, 6 H), 3.05 (s, 6 H), 2.89 (s, 6 H); CH_2CH_3, 1.61 (t, 7.3 Hz, 12 H), 1.50 (t, 7.3 Hz, 6 H), 1.43 (t, 7.4 Hz, 6 H); N–H, −3.40 (br s, 1 H), −3.55 (br s, 1 H). LSIMS: *m/e* 1363 (cluster, M^+), 1283 (cluster, $M^+ - py$), 1205 (cluster $M^+ + H - 2$ py). UV–vis (toluene/py): λ_{max} (log ϵ) 397 (5.15), 501 (4.24), 526 (4.25), 574 (3.67), 627 nm (3.27).

(Os)(H_2)DPB$(Py)_2$ (7). A solution of **3** (50 mg, 0.037 mmol) in pyridine (300 mL) was irradiated for 48 h in a quartz reaction vessel under argon atmosphere. The disappearance of the 538-nm band was monitored to determine the completion of the reaction. However, this osmium carbonylporphyrin band overlaps with a band assigned to the free-base porphyrin moiety, so even at completion there exists a weak shoulder band at 535 nm. The pyridine solution was evaporated and then worked up as described for **6** (44 mg, 82%). ^1H NMR (C_6D_6, ppm): H_{meso}, 9.84 (s, 2 H), 9.61 (s, 1 H), 8.12 (s, 1 H), 7.97 (s, 2 H); biphenylene, 7.02 (d, 6.9 Hz, 1 H), 6.90 (d, 6.9 Hz, 1 H), 6.76 (t, 6.5 Hz, 1 H), 6.66 (t, 6.5 Hz, 1 H), 6.60 (d, 6.8 Hz, 1 H), 6.44 (d, 6.9 Hz, 1 H); outer pyridine, H_p 4.84 (t, 6.4 Hz, 1 H), H_o 1.14 (d, 5.4 Hz, 2 H); inner pyridine, H_p 0.21 (t, 6.5 Hz, 1 H), H_m 0.04 (t, 6.7 Hz, 2 H), H_o 3.00 (d, 5.5 Hz, 2 H); CH_2CH_3, 3.96 (m, 4 H), 3.69–3.44 (m, 12 H), 3.35 (q, 7.5 Hz, 4 H); CH_3, 3.58 (s, 6 H), 3.56 (s, 6 H), 3.09 (s, 6 H), 2.89 (s, 6 H); CH_2CH_3, 1.63 (t, 7.5 Hz, 6 H), 1.56 (t, 7.4 Hz, 6 H), 1.47 (t, 7.6 Hz, 6 H), 1.43 (t, 7.6 Hz, 6 H); N–H, −3.31 (br s, 1 H), −3.46 (br s, 1 H). LSIMS: *m/e* 1452 (cluster, M^+), 1373 (cluster, $M^+ - py$), 1294 (cluster, $M^+ - 2$ py). UV–vis (toluene/py): λ_{max} (log ϵ) 393 (5.13), 409 sh (5.00), 480 sh (4.13), 513 (4.44), 535 sh (3.97), 573 (3.80), 627 nm (3.45).

$(Os)_2DPB(Py)_4$ (8). A solution of **4** (100 mg, 0.0590 mmol) in pyridine (400 mL) was irradiated in a quartz reaction vessel under an argon atmosphere until the 540-nm band had disappeared and then an additional 24 h. The workup procedure was similar to that described for **7** (77 mg, 73%). ^1H NMR (C_6D_6, ppm): H_{meso}, 8.55 (s, 2 H), 8.23 (s, 4 H); biphenylene, 6.90 (d, 6.7 Hz, 2 H), 6.67 (t, 7.6 Hz, 2 H), 6.52 (d, 6.5 Hz, 2 H); outer pyridine, H_p 4.94 (t, 2 H), H_m 4.11 (t, 6.8 Hz, 4 H), H_o 3.28 (d, 5.9 Hz, 4 H); inner pyridine, H_m 2.84 (t, 6.8 Hz, 4 H), H_o 2.70 (d, 5.9 Hz, 4 H); CH_2CH_3, 3.82–3.42 (m); CH_3, 3.73 (overlapping s), 3.00 (s, 12 H); CH_2CH_3, 1.63 (t, 7.4 Hz, 12 H), 1.52 (br s, 12 H). LSIMS: *m/e* 1798 (cluster, M^+). UV–vis (toluene/py): λ_{max} (log ϵ) 337 (4.77), 392 (5.23), 411 sh (4.76), 440 (4.32), 480 sh (4.47), 486 (4.48), 512 (4.81), 559 sh (4.02), 653 nm (3.32).

(Os)(Ru)DPB$(Py)_4$ (9). A solution of **5** (20 mg, 0.013 mmol) in pyridine (300 mL) was irradiated in a quartz reaction vessel until the absorbance ratio of the 513/524 visible bands equaled 1.251 (≈48 h) and then an additional 12 h. The pyridine solution was evaporated and the residue heated under vacuum (70 °C, 10^{-2} Torr) for 12 h and then taken into the glovebox. The solid was dissolved in toluene/THF (2/1) and chromatographed (Al_2O_3, 0.5 × 5 cm) eluting with the same solvent mixture. The orange eluent was evaporated and then redissolved in toluene (1 mL) and filtered through a glass wool plug. This solution was concentrated (0.3 mL), 2 drops of pyridine were added, and then CH_3OH (1.5 mL) was layered over the top to crystallize the product upon cooling (−20 °C). The dark orange solid was vacuum filtered, washed with CH_3OH (1 mL), and dried under vacuum (19 mg, 84%). ^1H NMR (C_6D_6, ppm): H_{meso}, 9.42 (s, 1 H), 9.20 (br s, 2 H), 8.53 (s 1 H), 8.19 (br s, 2 H); biphenylene, 6.95 and 6.94 (overlapping d, 2 H), 6.69 (t, 7.3 Hz, 1 H), 6.62 (t, 7.3 Hz, 1 H), 6.52 (d, 8.3 Hz, 1 H), 6.33 (d, 8.0 Hz, 1 H); outer pyridines, H_p 4.94 (t, 1 H) and 4.71 (t, 1 H), H_o 3.26 (d, 5.4 Hz, 2 H); inner pyridines, H_m 2.81 (t, 6.6 Hz, 2 H) and 2.45 (t, 7.1 Hz, 2 H), H_o 2.54 (d, 5.3 Hz, 2 H) and 2.10 (d, 5.3 Hz, 2 H); CH_2CH_3, 4.09 (q, 4 H), 3.85–3.35 (overlapping m); CH_3, 3.76 and 3.65 (overlapping s), 2.99 (s, 6 H), 2.97 (s, 6 H); CH_2CH_3, 1.60 (t), 1.70 (t), 1.56 (overlapping t). LSIMS: *m/e* 1709 (cluster, M^+), 1630 (cluster, $M^+ - py$), 1551 (cluster, $M^+ - 2$ py), 1393 (cluster, $M^+ - 4$ py). UV–vis (toluene/py): λ_{max} (log ϵ) 344 (4.73), 393 (5.24), 412 sh (5.02), 445 (4.42), 478 sh (4.39), 490 (4.46), 513 (4.69), 524 (4.62), 568 sh (3.84), 650 nm (3.31).

$(Os)_2DPB$ (10). In the glovebox, **8** (50 mg, 0.028 mmol) was dissolved in benzene (1.5 mL) and added to a pyrolysis tube equipped with a vacuum adapter. The sealed tube was removed from the glovebox, and the dark orange solution was quickly frozen with a liquid-nitrogen bath. Under vacuum (10^{-2} Torr), the solid solution was warmed to 0 °C. The benzene sublimed away to yield an amorphous orange powder. Vacuum pyrolysis (230 °C, 1 × 10^{-5} Torr) for 12 h gave a quantitative yield of **10** as an air-sensitive, brown solid (40 mg, 97%). FABMS: *m/e* 1482 (cluster, M^+). UV–vis (toluene): λ_{max} (log ϵ) 362 (4.89), 529 sh (3.90), 625 sh (3.59), 671 nm (3.31).

(Os)(Ru)DPB (11). Lyophilization of a benzene solution of **9** (50 mg, 0.029 mmol) by the procedure described in the synthesis of **10** yielded a red-orange solid. Under vacuum (1 × 10^{-5} Torr), the pyrolysis tube was dipped into an heated silicone oil bath (230 °C), and heating was continued for 12 h to yield an air-sensitive, dark brown solid (40 mg, 98%). FABMS: *m/e* 1393 (cluster, M^+). UV–vis (toluene): λ_{max} (log ϵ) 372 (5.00), 485 (4.18), 677 nm (3.57).

Results and Discussion

In order to take advantage of the cofacial bis(porphyrin)'s ability to hold two different metals at close proximity, a synthetic methodology had to be developed to monometalate the bis(porphyrin) with a 4d or 5d metal. The other free-base porphyrin could then be metalated with a different metal to yield the desired heterobimetallic complex. The most direct approach is to titrate the bis(free-base)bis(porphyrin)(H_4DPB) with 0.5 equiv of the 4d or 5d metal. However, initial attempts with ruthenium and osmium were unsuccessful in producing high yields of the mo-

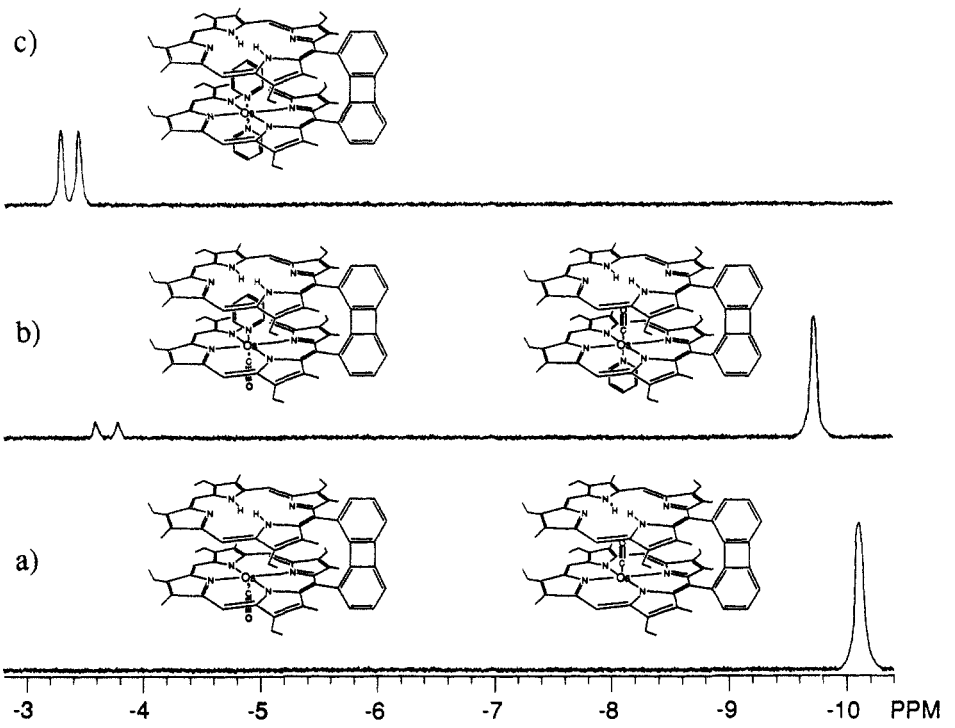

Figure 3. (a) High-field region of the ^{1}H NMR spectrum of (Os)(H_2)DPB(CO)(CH_3OH) showing the N–H resonance of the free-base porphyrin moiety. The methanol ligand has been omitted in the structures of the two isomers. (b) N–H resonances of the two isomers of (Os)(H_2)DPB(CO)(Py). (c) N–H resonance for (Os)(H_2)DPB(Py)$_2$.

nometalated product[10] so another approach was investigated (eq 2). This method has been described qualitatively for the prep-

$$H_4DPB + Zn(O_2CCH_3)_2 \rightarrow (Zn)(H_2)DPB \xrightarrow{M_3(CO)_{12}} \underset{\mathbf{1}}{} (M^{II})(Zn)DPB(CO)$$

$$(M^{II})(Zn)DPB(CO) + 2HCl \xrightarrow{CH_3OH} (M^{II})(H_2)DPB(CO)(CH_3OH) \quad (2)$$

2, M = Ru
3, M = Os

aration of 3d heterobimetallic compounds using an anthracene-bridged bis(porphyrin).[5b] One porphyrin is protected by metallation with Zn(II) to yield the (Zn)(H_2)DPB complex. This is accomplished by titrating a boiling CH_2Cl_2 solution of H_4DPB with slightly less than 0.5 equiv of zinc acetate dissolved in methanol. The free-base porphyrin of this complex can then be metalated with ruthenium or osmium to yield (Ru^{II})(Zn)DPB(CO) or (Os^{II})(Zn)DPB(CO), respectively. Treatment with 6 M aqueous HCl then demetalates the zinc porphyrin, but not the ruthenium or osmium porphyrin, to yield the monometalated ruthenium (**2**) and osmium (**3**) bis(porphyrin) complexes. Hence, the zinc ion serves as the inorganic equivalent of a protecting group in synthetic organic chemistry. The synthetic procedure shown in eq 2 should be applicable to the monometalation of H_4DPB with every transition metal since these metals are not as labile toward acid as the zinc ion.[11] Although the protection method is more lengthy than the direct approach mentioned above, it allows the preparation of the monometalated porphyrin in good yields without any of the dimetalated bis(porphyrin) byproduct. This byproduct may otherwise represent a significant waste of the valuable H_4DPB compound.

The monometalated ruthenium (**2**) and osmium (**3**) bis(porphyrins) both possess an axially coordinated carbonyl ligand as determined from infrared and mass spectral data. The frequencies of the infrared carbonyl bands are similar to those of the corresponding mononuclear metalloporphyrin complexes [i.e., Ru(OEP)(CO)(CH_3OH)]. However, the ^{1}H NMR spectra reveal that each of these compounds exists as two geometric isomers. This can be determined by comparing the chemical shifts of the N–H resonance(s) of the free-base porphyrin moiety for (M)(H_2)DPB(CO)(CH_3OH) and the analogous pyridine-substituted complexes, (M)(H_2)DPB(CO)(Py) (M = Ru or Os).[12] Spectra a and b of Figure 3, respectively, show the high-field resonances of the osmium compounds. The CH_3OH complex **3** has one N–H resonance at −10.13 ppm, whereas, the pyridine complex has two N–H resonances. One is observed at −9.70 ppm (similar to **3**), and the other is shifted downfield and centered at −3.7 ppm.[13] Coordination of the pyridine ligand outside of the bis(porphyrin) cavity should have little effect on the chemical shift of the N–H resonance. However, three factors could contribute to a downfield shift of this resonance should the pyridine ligand be coordinated within the bis(porphyrin) cavity. If the pyridine ligand was oriented within the cavity as drawn in the bis(porphyrin) structure of Figure 3b, then the magnetic anisotropy of this ligand would contribute to a downfield shift of the N–H resonance. Likewise, it is reasonable to assume that placement of a large aromatic ligand (pyridine) in the highly shielding region of the bis(porphyrin) structure will cause a decrease in the ring current experienced by the N–H proton. The ring current associated with the pyridine ligand should oppose that of the two porphyrins since the π orbitals would be expected to lie roughly orthogonal to each other. Structural factors may also contribute to the differences in chemical shift of the N–H resonances, but any conclusions with the present data would be highly speculative.[14]

(10) Unlike metalations with 3d metals, 4d and 5d transition metals typically require an excess of the metal source for high-yield metalations of synthetic porphyrins.

(11) Buchler, J. W. *Porphyrins and Metalloporphyrins*; Smith, K. M.; Ed.; Elsevier: New York, NY, 1975; p 195.

(12) This information cannot be inferred from an analysis of the other porphyrin resonances. (Ru^{II})(H_2)DPB(CO)(Py) [LSIMS: *m/e* 1312 (cluster, M^+)] and (Os^{II})(H_2)DPB(CO)(Py) [LSIMS: *m/e* 1401 (cluster, M^+)] may be prepared by heating a pyridine solution of the corresponding CH_3OH complexes **2** and **3** at reflux for approximately 15 min. The ^{1}H NMR spectra of the pyridine complexes are very complicated. For example, seven of a possible eight H_{meso} resonances are observed for the (Os)(H_2)DPB(CO)(Py) complex.

(13) The N–H protons for the DPB compounds [H_4DPB and (Zn)(H_2)-DPB] often appear as two signals instead of one, indicating the loss of the C_2 axis of symmetry bisecting the biphenylene structure. This may be caused by porphyrin skeletal distortions similar to those found in the crystal structure of (Cu)$_2$DPB. See: Fillers, J. P.; Ravichandran, K. G.; Abdalmuhdi, I.; Tulinsky, A.; Chang, C. K. *J. Am. Chem. Soc.* **1986**, *108*, 417.

Further evidence for the existence of isomers in the $(M)(H_2)$-DPB(CO)(py) compounds can be obtained when the carbonyl ligand in **3** is substituted with pyridine. Upon UV irradiation, this compound is converted to $(Os)(H_2)DPB(Py)_2$ (**7**). The N–H resonance is centered at −3.4 ppm (Figure 3c), and the upfield N–H resonance for **3** at ≈ −10 ppm is no longer observed. The ^1H NMR spectrum of **7** is consistent with a single isomer, but two different sets of pyridine resonances are observed. One set has chemical shifts similar to those of $Os^{II}(OEP)(Py)_2$, whereas, the other set is shifted 0.3–4.8 ppm upfield. This observation is evidence for *trans* axial pyridine ligands with one coordinated *outside* and one *inside* the diporphyrin cavity, as shown in Figure 3c.[15] Hence, each N–H resonance for $(Os)(H_2)DPB(CO)(Py)$ can be assigned with respect to the axial position of the pyridine ligand, and integration of the two N–H resonances gives the relative amounts of each geometric isomer. These experiments show that both the ruthenium (**2**) and osmium (**3**) monometalated complexes have approximately 80% of the carbonyl ligands coordinated within the bis(porphyrin) cavity. This ratio likely reflects a kinetic rather than a thermodynamic stability toward substitution.

The diosmium and (osmium)(ruthenium) bis(porphyrin) carbonyl complexes may be prepared by the reactions shown in eq 3 and 4, respectively. Again, both compounds possess two carbonyl ligands as determined by mass spectroscopy. Only one infrared carbonyl band is observed for the $(Os^{II})_2DPB(CO)_2(Py)_2$ compound (**4**), and the frequency is similar to that of the osmium monometalated bis(porphyrin) (**3**). This indicates that each carbonyl ligand is coordinated to only one metal. Earlier, this same observation for $(Ru^{II})_2DPB(CO)_2(CH_3OH)_2$ was thought to also imply that both carbonyl ligands were located outside of the bis(porphyrin) cavity.[16] However, two sets of coordinated pyridine resonances are observed for the diosmium complex **4** so isomers must exist similar to the monometalated bis(porphyrins) (**2** and **3**). The infrared spectrum of the heterobimetallic complex **5** also suggests a mixture of isomers as three carbonyl bands at 1931, 1905, and 1865 cm^{-1} are observed. The latter two bands are weaker in intensity than the former. The 1931-cm^{-1} band is assigned to the ruthenium carbonyl by comparison with the frequency of the ruthenium monometalated bis(porphyrin) (**2**). However, the other two bands are not assignable since intramolecular bridging of this ligand between the two metals (i.e., Ru$C\equiv O\cdots$Os or Os$C\equiv O\cdots$Ru), as well as an unbridged osmium carbonyl, could give stretching bands in this frequency region. Both of these bis(porphyrin) compounds **4** and **5** are mildly air-sensitive when in solution, and the diosmium complex oxidizes immediately when solutions are heated in air. This is unexpected since similar mononuclear ruthenium and osmium carbonyl porphyrins, such as $Os^{II}(OEP)(CO)(CH_3OH)$ and the monometallic bis(porphyrins) (**2** and **3**), show little oxygen sensitivity. This increased sensitivity is evidently caused by the close proximity of both metals, but the exact nature of these oxidation reactions remain unclear.

The carbonyl ligands of the bimetallic bis(porphyrins) **4** and **5** can be substituted with pyridine upon UV irradiation (eq 5 and 6) similar to the corresponding ruthenium and osmium OEP compounds.[17] ^1H NMR and mass spectral data confirm the presence of four pyridine ligands per bimetallic bis(porphyrin). Two sets of pyridine resonances of equal intensity are observed for the diosmium complex **8**, which is consistent with two of these ligands being coordinated to each metal and a *trans* arrangement of each osmium dipyridine fragment. Hence, two pyridine ligands are coordinated *outside* and two *inside* the bis(porphyrin) cavity. Spectroscopic evidence for a similar arrangement of these axial ligands was also found for the analogous ruthenium complex, $(Ru^{II})_2DPB(Py)_4$.[16] The ^1H NMR spectrum of the (osmium)-(ruthenium) bis(porphyrin) **9** is consistent with a single isomer, but too many of the pyridine resonances overlap with other porphyrin resonances to establish rigorously whether these ligands are disposed like those of the diosmium complex.[8] However, resonances are observed for pyridines coordinated inside and outside of the bis(porphyrin) cavity. It is rather surprising that the DPB cavity can accommodate two pyridine ligands since there is only a 3.5-Å mean distance between the two porphyrin planes in the solid-state structure of $(Cu)_2DPB$.[13] The two pyridine ligands within the cavity must tilt away from the pseudo 4-fold axis of symmetry at each metal if the same distance is also present in solution. Flexibility in the DPB structure may also allow for an increase in the size of the bis(porphyrin) cavity.

Vacuum pyrolysis of the orange tetrapyridine complexes by the solid-state procedure described for the analogous Ru DPB compound[18] yields new air-sensitive, brown compounds. ^1H NMR and mass spectral data support the product formulations shown in eq 7 and 8, indicating the loss of all four pyridine ligands for each bis(porphyrin) complex. The sharp ^1H NMR resonances of the diosmium **10** and (osmium)(ruthenium) **11** products are paramagnetically shifted and are shown in Figures 4 and 5. Paramagnetism can be predicted for two d^6 metal ions forming a metal–metal double bond with the electronic configuration $\sigma^2\pi^4\delta^2\delta^{*2}\pi^{*2}$. The assignments of the $(Os)_2DPB$ and (Os)-(Ru)DPB resonances in Table I are based upon spin–spin splitting patterns, integration, and decoupling experiments, as well as a comparison of the chemical shifts to those of the osmium and ruthenium OEP dimers. Each set of biphenylene resonances for (Os)(Ru)DPB are determined from decoupling experiments (irradiation of each H_m triplet) and are tentatively assigned to either the osmium or ruthenium porphyrin fragments based upon a comparison of the chemical shifts of those of the $(Ru)_2DPB$ and $(Os)_2DPB$ complexes. The biphenylene H_o and H_p resonances are not assigned. Both ^1H NMR spectra are consistent with either bis(porphyrin) structures with intramolecular metal–metal bonds or polymeric diporphyrin structures with intermolecular metal–metal bonds, [i.e., $(=Os(DPB)Os=)_n$, with a very large value(s) for n].[19] The good solubility of both products is support for

$$H_4DPB + Os_3(CO)_{12} \xrightarrow{Py} \underset{\mathbf{4}}{(Os^{II})_2DPB(CO)_2(Py)_2} \quad (3)$$

$$(Ru^{II})(H_2)DPB(CO)(CH_3OH) + Os_3(CO)_{12} \xrightarrow{CH_3OH} \underset{\mathbf{5}}{(Os^{II})(Ru^{II})DPB(CO)_2(CH_3OH)_2} \quad (4)$$

$$(Os^{II})_2DPB(CO)_2(Py)_2 \xrightarrow[Py]{UV\ h\nu} \underset{\mathbf{8}}{(Os^{II})_2DPB(Py)_4} \quad (5)$$

$$(Os^{II})(Ru^{II})DPB(CO)_2(CH_3OH)_2 \xrightarrow[Py]{UV\ h\nu} \underset{\mathbf{9}}{(Os^{II})(Ru^{II})DPB(Py)_4} \quad (6)$$

$$(Os^{II})_2DPB(Py)_4 \xrightarrow[10^{-5}\ Torr]{230\ ^\circ C} (Os^{II})_2DPB \quad (7)$$

$$(Os^{II})(Ru^{II})DPB(Py)_4 \xrightarrow[10^{-5}\ Torr]{230\ ^\circ C} (Os^{II})(Ru^{II})DPB \quad (8)$$

(14) Distortions in the cofacial bis(porphyrin) structure may include porphyrin–porphyrin slippage, porphyrin skeletal distortions away from planarity, larger porphyrin–porphyrin bite angle, etc.

(15) A pyridine coordinated within the cavity would experience the ring current of two porphyrins whereas a pyridine coordinated outside would experience the ring current of only one porphyrin. Hence, the resonances of the pyridine within the bis(porphyrin) cavity should appear at higher field than those of the pyridine outside of the cavity.

(16) Collman, J. P.; Kim, K.; Leidner, C. R. *Inorg. Chem.* **1987**, *26*, 1152.

(17) (a) Hopf, F. R.; O'Brien, T.; Scheidt, W.; Whitten, D. *J. Am. Chem. Soc.* **1975**, *97*, 277. (b) Antipas, A.; Buchler, J.; Gouterman, M.; Smith, P. *J. Am. Chem. Soc.* **1978**, *100*, 3015.

(18) See ref 15. This temperature is slightly higher than the temperature (210 °C) required for the $Os(OEP)(Py)_2$ and $Ru(OEP)(Py)_2$ compounds. Vacuum pyrolysis of $(Os)_2DPB(Py)_4$ and (Os)(Ru)$DPB(Py)_4$ at this lower temperature results in an incomplete reaction even after 48 h. This observation may also be evidence for pyridine ligands coordinated within the DPB cavity.

(19) The high molecular weights of (Os)(Ru)DPB and $(Os)_2DPB$ and low solubilities of porphyrin complexes in general make solution molecular weight measurements futile. Also, oligomeric species (small n) would give a more complex ^1H NMR spectrum than is observed so such compounds can be ruled out.

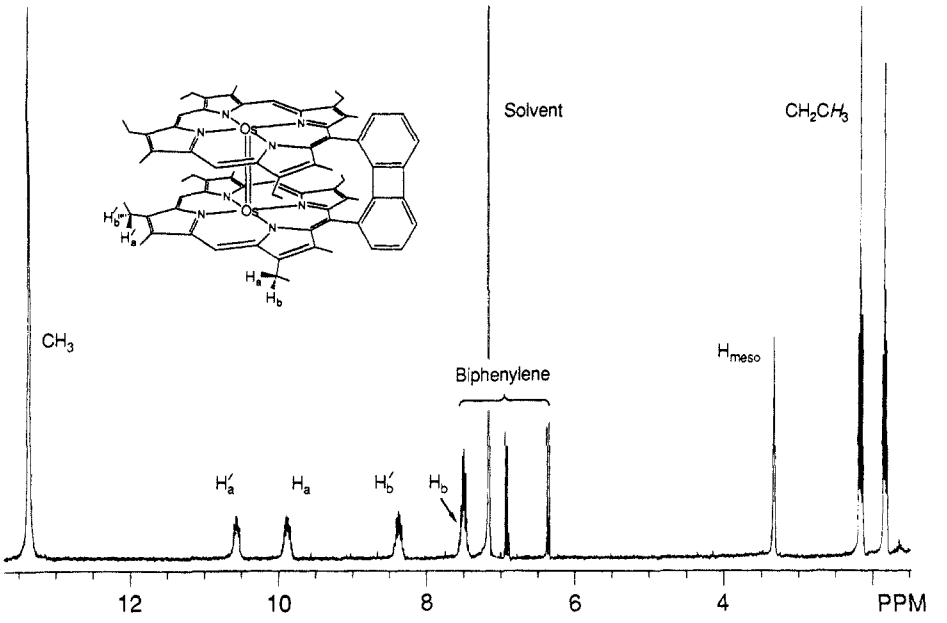

Figure 4. ^1H NMR spectrum of $(Os)_2DPB$ in C_6D_6 at 21 °C.

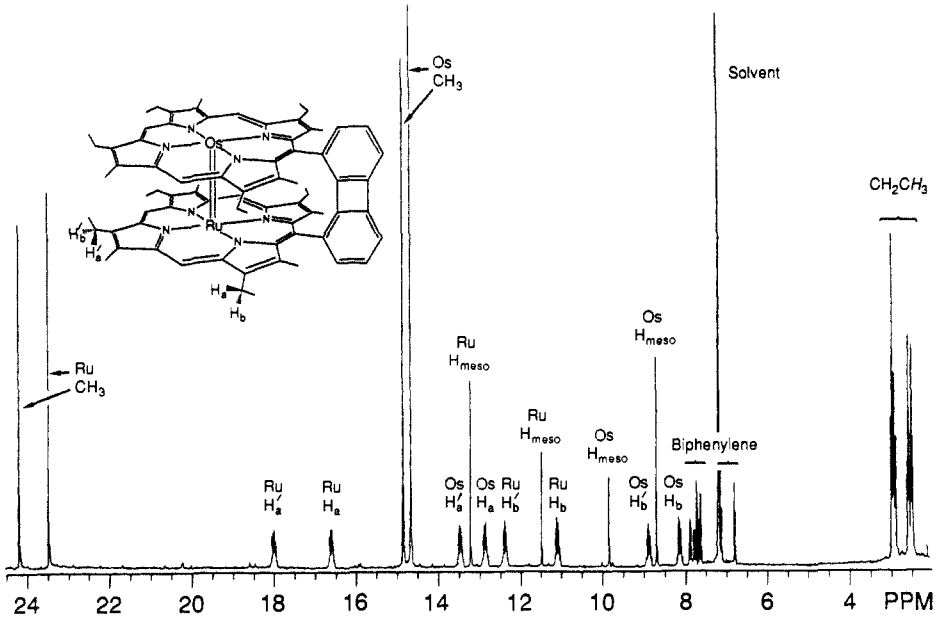

Figure 5. ^1H NMR spectrum of (Os)(Ru)DPB in C_6D_6 at 21 °C.

Table I. ^1H NMR Data for Neutral Ruthenium and Osmium Metal–Metal Bonded Porphyrin Dimers in C_6D_6 at 21 °C

complex	H_{meso}	CH_2CH_3 H_a	CH_2CH_3 H_b	CH_2CH_3	CH_3	biphenylene
$[Ru(OEP)]_2$	10.14	25.51	11.0	3.42		
$(Ru)_2DPB$	20.34 18.71	24.58 22.66	12.16 10.56	3.70 3.31	31.54 29.89	7.84 7.47[a]
$[Os(OEP)]_2$	−1.08	11.56	7.83	1.97		
$(Os)_2DPB$[b]	3.33 3.31	10.56 9.87	8.36 7.51	2.15 1.82	13.36	7.49 6.92 6.35
[(OEP)OsRu(OEP)]						
Os(P) fragment	3.01	13.47	8.18	2.6		
Ru(P) fragment	6.08	19.98	11.18	2.6		
(Os)(Ru)DPB						
Os(P) fragment[c]	9.79 8.65	13.43 12.81	8.84 8.10	2.87 2.45	14.80 14.61	7.84 7.68 6.75
Ru(P) fragment[d]	13.17 11.43	17.94 16.56	12.34 11.06	2.93 2.53	24.16 23.44	7.59 7.74 7.09

[a] The H_o and H_p resonances overlap. [b] Assignments are as follows across columns: (s, 2 H), (s, 4 H), (m, 4 H), (m, 4 H), (m, 4 H), (overlapping m, 4 H), (t, 7.6 Hz, 12 H), (t, 7.6 Hz, 12 H), both methyl resonances overlap (s, 24 H). H_m (overlapping t, 7.6 Hz, 2 H), (d, 6.8 Hz, 2 H), (d, 8.2 Hz, 2 H). [c] Assignments are as follows across columns: (s, 1 H), (s, 2 H), (m, 2 H), (m, 2 H), (m, 2 H), (m, 2 H), (t, 7.5 Hz, 6 H), (t, 7.6 Hz, 6 H), (s, 6 H), (s, 6 H), H_m (t, 7.3 Hz, 1 H), (d, 7.3 Hz, 1 H), (d, 7.3 Hz, 1 H); resonance in column 8 is coupled to those in columns 4 and 7; resonance in column 9 is coupled to those in columns 5 and 6. [d] Assignments are as follows across columns: (s, 2 H), (s, 4 H), (m, 2 H), (m, 2 H), (m, 2 H), (m, 2 H), (t, 7.2 Hz, 6 H), (t, 7.5 Hz, 6 H), (s, 6 H), (s, 6 H), H_m (t, 7.3 Hz, 1 H), (d, 6.0 Hz, 1 H), (d, 7.4 Hz, 1 H); resonance in column 8 is coupled to those in columns 4 and 7; resonance in column 9 is coupled to those in columns 5 and 6.

Table II. Solution Magnetic Moments[a] for Ruthenium and Osmium Metal–Metal Bonded Porphyrin Dimers in C_6D_6 at 21 °C

compd	μ_{eff}	compd	μ_{eff}
$[Ru(OEP)]_2$	2.3 ± 0.2	$(Os)_2DPB$	1.0 ± 0.3
$[Os(OEP)]_2$	1.2 ± 0.3	(Os)(Ru)DPB	1.3 ± 0.3
$(Ru)_2DPB$[b]	2.2 ± 0.2		

[a] Calculated as μ_B per dimer. [b] The moment for this complex was incorrectly reported as 2.6 μ_B due to an error in the calculation.[6]

discrete dimers with intramolecular metal–metal bonds. Also, the UV–visible spectra of (Os)(Ru)DPB and $(Os)_2DPB$ feature broadened Soret and Q-bands like those previously observed for $[Ru(OEP)]_2$[20] and $[Os(OEP)]_2$.[21]

In comparison to the resonances of $(Os_2)DPB$ and $(Ru)_2DPB$, significant chemical shift differences (6–7 ppm) are observed for the H_{meso}, CH_2CH_3, and CH_3 resonances in both the osmium and ruthenium porphyrin fragments of (Os)(Ru)DPB. However, these chemical shift differences seem reasonable[22] and may simply reflect differences in the relative magnitude of the dipolar (through-space interactions of metal unpaired electrons with ligand protons) and Fermi (delocalization of unpaired spin density at a ligand proton via covalent metal–ligand interactions) contributions to the paramagnetic shifts for the Ru=Ru, Os=Os, and Os=Ru species.[23] To demonstrate this contention explicitly, a quantitative analysis of each ^1H NMR spectrum to delineate the relative magnitude of these two types of paramagnetic contributions would have to be performed similar to that previously determined for $[Ru(OEP)]_2$.[20] This analysis would, however, require more structural information and an assignment of all biphenylene resonances.[20,23] Preliminary attempts to grow single crystals of (Os)(Ru)DPB and $(Os)_2DPB$ by slow evaporation of benzene solutions were unsuccessful.

Solution magnetic moments for $(Ru)_2DPB$, $(Os)_2DPB$, and (Os)(Ru)DPB at 21 °C are listed in Table II. The magnitude of the moments for $(Ru)_2DPB$ and $(Os)_2DPB$, are within experimental error, similar to the moments for the respective $[Ru(OEP)]_2$ and $[Os(OEP)]_2$ compounds. The magnetic moment for (Os)(Ru)DPB is intermediate between that measured for $(Os)_2DPB$ and $(Ru)_2DPB$ but more closely approaches the value for the diosmium compound. These moments are reduced from the free-spin value for two unpaired electrons but may still be consistent with a $\sigma^2\pi^4\delta^2\delta^{*2}\pi^{*2}$ electronic configuration. Earlier we proposed an $^3A_{2g}$ ground state (the paramagnetic state derived from the half-filled π^* MO) for the $[Ru(Por)]_2$ compounds based upon the observed Curie law behavior of chemical shifts for the porphyrin ^1H resonances.[20] However, magnetic susceptibility measurements of $[Ru(OEP)]_2$ in the solid state that followed indicate that the effective moment of this dimer decreases as the temperature is lowered and nearly reaches 0 μ_B at liquid-helium temperatures.[24] This solid-state data could be interpreted in two ways. Either intermolecular antiferromagnetic interactions become important in the solid state at low temperatures or a nonmagnetic state is at slightly lower energy (within kT or ≈200 cm^{-1}) than the triplet state, which gives rise to the paramagnetism at room temperature. We initially favored the former explanation as the spin equilibria seemed to contradict the solution NMR measurements. However, if the energy difference between these levels is ≤kT, then the Boltzmann population of the two states may not vary significantly over the high absolute temperatures (180–370 K) of the NMR measurements. Under these circumstances, the nonlinear region of the Curie plots of chemical shift versus T^{-1} for the $[Ru(Por)]_2$ compounds may only be observed at lower temperatures than 180 K. Experimental reasons (solubility, solvent freezing points, and instrument design) present lower temperature studies of the solution magnetic properties of these dimers by NMR to test this hypothesis. However, to our knowledge this would be the only way to reconcile the solution and solid-state magnetic data is favor of the explanation involving a thermal equilibria between nonmagnetic and paramagnetic states.

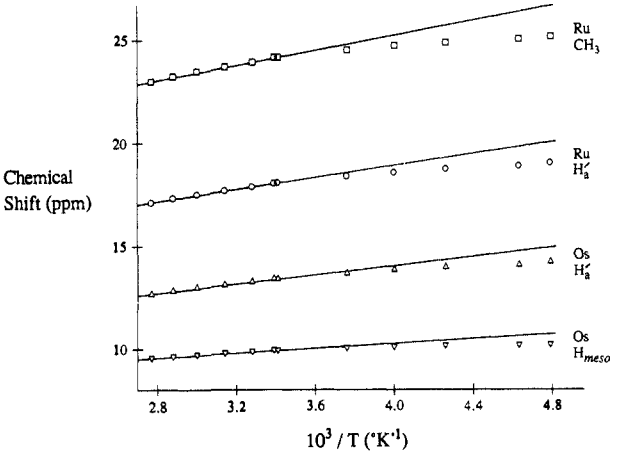

Figure 6. Curie plot for selected resonances of (Os)(Ru)DPB in $C_6D_5CD_3$ between −65 and +100 °C.

This reexamination of the solution NMR data became necessary due to a recent magnetic susceptibility study of diruthenium(II) tetraacetate by Cotton, Miskowski, and Zhong.[25] These researchers report similar solid-state magnetic properties for this compound as those found for $[Ru(OEP)]_2$. The magnetic moment for $Ru_2(O_2CCH_3)_4$ at room temperature, 2.8 μ_B, decreases to 0.6 μ_B at 5 K. Although the details of their analysis will not be repeated here, intermolecular antiferromagnetic interactions have been eliminated as the primary cause of the decreasing moments as the temperature is lowered. Instead, they present strong evidence for a zero-field splitting of the $^3A_{2g}$ state to yield the nonmagnetic A_{1g} triplet ground state ($m_s = 0$) and a slightly higher energy (≈240 cm^{-1}) E_g triplet state ($m_s = \pm 1$). We also intend to apply their model to the solid-state data for $[Ru(OEP)]_2$ and $[Os(OEP)]_2$.

The temperature dependence for all resonances of (Os)(Ru)-DPB in $C_6D_5CD_3$ was examined to investigate whether any solution evidence for a similar equilibrium between A_{1g} and E_g states could be obtained for this new compound. The chemical shift changes over the temperature range investigated (−65 to +95 °C)[26] are rather small (≤2.8 ppm) so the accuracy of this analysis is limited. Selected resonances giving rise to the largest chemical shift changes are shown in Figure 6. Virtually all the resonances, including those of the biphenylene structure, are found to exhibit a low-temperature, upfield deviation from the straight line drawn through the high-temperature data points. Although this nonlinear Curie behavior would be consistent with the thermal population of two magnetic states as discussed above, upfield deviations such as these have been observed previously in intermediate spin (S = 1), four-coordinate ferrous porphyrins[27] and the β-pyrrolic resonance $[Ru(TPP)]_2$.[20] The deviations in the latter cases were simply attributed to aggregation as the temperature is lowered. The diamagnetic ring current of the porphyrin π electrons presumably shifts the resonances upfield. The chemical shifts of the (Os)(Ru)DPB resonances are only slightly concentration de-

(20) Collman, J. P.; Barnes, C. E.; Sweptson, P. N.; Ibers, J. A. *J. Am. Chem. Soc.* **1984**, *106*, 3500.
(21) Collman, J. P.; Barnes, C. E.; Woo, L. K. *Proc. Natl. Acad. Sci. U.S.A.* **1983**, *80*, 7684.
(22) The chemical shift values for the H_{meso}, CH_2CH_3, and CH_3 resonances of the Ru(P) and Os(P) fragments of (Os)(Ru)DPB are simply intermediate between the chemical shift values for the analogous resonances of $(Ru)_2DPB$ and $(Os)_2DPB$, respectively. This intermediacy of chemical shifts might be expected for an intermediate complex. Note that significant differences only occur for those resonances with large differences between $(Ru)_2DPB$ and $(Os)_2DPB$ ($\Delta\delta$ H_{meso} ≈ 16 ppm; $\Delta\delta$ H_a ≈ 13.5 ppm; $\Delta\delta$ CH_3 ≈ 17 ppm).
(23) La Mar, G. N.; Walker (Jensen), F. A. *The Porphyrins*; Dolphin, D., Ed.; Academic Press: San Francisco, CA, 1979; Vol. IV, p 61.
(24) Collman, J. P.; Miller, J. S.; Barnes, C. E., unpublished results.
(25) Cotton, F. A.; Miskowski, V. M.; Zhong, B., submitted for publication of *J. Am. Chem. Soc.*
(26) Below −65 °C the resonances broaden significantly. This is likely due to slower tumbling of the large (Os)(Ru)DPB molecule as the solvent viscosity increases upon cooling.
(27) Goff, H.; La Mar, G. N.; Reed, C. A. *J. Am. Chem. Soc.* **1977**, *99*, 3641.

pendent (±0.01 ppm)[28] so this can be excluded as the dominate cause for the low-temperature deviations. Hence, simultaneous population of two states within this temperature range is consistent with the present data, but solid-state magnetic susceptibility measurements are required to prove this conclusively.

Conclusion

Heterobimetallic DPB complexes for all possible transition-metal combinations appear to be accessible with this straightforward, albeit lengthy, synthetic procedure. These developments may then lead to the preparation of porphyrin dimers with heteronuclear multiple bonds between 3d and 5d metals of the same triad, or more interestingly, between metals from different triads. In this study, we have chosen a trivial example of a heteronuclear metal-metal multiple bond, Os≡Ru, to demonstrate that the cofacial bis(porphyrin) ligand can control the reaction stoichiometry and facilitates the formation of the intramolecular metal-metal bond. The stability of low oxidation states and the coordination chemistry necessary for the formation of the metal-metal bond (eq 6 and 8) are very similar for these two metals. This has made all the synthetic steps exactly analogous to those of the osmium and ruthenium complexes and allowed for two convergent steps. The syntheses for more interesting combintions, such as early-late transition metals (i.e., Mo≡Ru), will probably not be as straightforward. The disparity between low oxidation state stabilities and the coordination chemistry of the two metalloporphyrins may still frustrate the synthesis. However, we nevertheless view this general synthetic procedure as an important step in the preparation of complexes with heteronuclear metal-metal multiple bonds.

We also anticipate benefits from these results in the area of electrocatalysis. The ability to prepare heterodinuclear DPB complexes with a 4d or 5d metal known to bind dinitrogen and another metal to activate it toward multielectron reduction should facilitate the survey of possible catalysts for this challenging catalytic reaction.

Acknowledgment. This work was supported by the National Science Foundation (Grant CHE83-18512). The NMR instrument was also funded by the National Science Foundation (Grant CHE81-09064). We thank Pat Bethel for LSI and FD mass spectral analyses of the new compounds at the Mass Spectroscopy Facility (A. L. Burlingame, Director) at the University of California, San Francisco, which is supported by the NIH Division of Research Resources, Grant RR01614, and Yunkyoung Ha for some assistance in the preparation of the latter compounds. This work is dedicated to J.M.G.'s father, James H. Garner.

(28) The maximum solubility of (Os)(Ru)DPB in benzene is approximately 3 mg/mL so the concentration range investigated was 0.2-0.7 mM.

ESR of Homo- and Heteroleptic Mono- and Dinuclear Tris(α-diimine)ruthenium Radical Complexes

Wolfgang Kaim,* Sylvia Ernst,[1] and Volker Kasack

Contribution from the Institut für Anorganische Chemie, Universität Stuttgart, Pfaffenwaldring 55, D-7000 Stuttgart 80, West Germany. *Received March 1, 1989*

Abstract: A comprehensive ESR study of 11 mononuclear and 5 dinuclear singly reduced tris(α-diimine)ruthenium(II) complexes of the general formulas $[(L)_3Ru]^{\bullet+}$, $[(L)(bpy)_2Ru]^{\bullet+}$, and $[(bpy)_2Ru(\mu\text{-}L)Ru(bpy)_2]^{\bullet3+}$ (bpy, 2,2'-bipyridine; L, other α-diimine) shows a variety of g factors and spectral resolution. All paramagnetic species are true anion-radical complexes with little g anisotropy and relatively small but characteristically positive differences g(ligand radical) − g(complex). The variations correlate with the calculated properties of the ligands and with spectroscopic and electrochemical data for the diamagnetic precursor complexes. In particular, the g shifts depend (i) on the extent of metal-ligand interaction and (ii) on the energy differences between the singly occupied and neighboring unoccupied or completely filled orbitals. Virtually complete localization of the unpaired electron on the better π-accepting ligand L has been established for the mono- and dinuclear heteroleptic systems, while fast spin exchange on the ESR time scale is evident from the ESR line width of all singly reduced homoleptic complexes.

The problem of (de)localization has been intensely debated in two areas of ruthenium ammine chemistry: One area has been the metal-metal interaction in the Creutz-Taube ion[2a] and related metal-metal mixed-valent species;[2] the other controversy surrounds the ligand-ligand mixed valency in reduced[3] or MLCT excited states[4] of tris(α-diimine)ruthenium complexes. Molecular ions such as $[Ru(bpy)_3]^{2+}$ are reversibly reduced[5,6] to anion-radical complexes (eq 1);[3a,b,7] the enormous attention devoted to this[4] and related complexes[5,8] stems from their use as photosensitizers, e.g., in water activation processes.[9]

(1) Present address: Beilstein-Institut fuer Organische Chemie, D-6000 Frankfurt/Main, West Germany.

(2) (a) Creutz, C.; Taube, H. *J. Am. Chem. Soc.* **1969**, *91*, 3988; **1973**, *95*, 1086. (b) Creutz, C. *Prog. Inorg. Chem.* **1983**, *30*, 1. (c) Richardson, D. E.; Taube, H. *Coord. Chem. Rev.* **1984**, *60*, 107. (d) Ernst, S.; Kasack, V.; Kaim, W. *Inorg. Chem.* **1988**, *27*, 1146.

(3) (a) Motten, A. G.; Hanck, K. W.; DeArmond, M. K. *Chem. Phys. Lett.* **1981**, *79*, 541. (b) Morris, D. E.; Hanck, K. W.; DeArmond, M. K. *J. Am. Chem. Soc.* **1983**, *105*, 3032. (c) *J. Electroanal. Chem.* **1983**, *149*, 115. (d) *Inorg. Chem.* **1985**, *24*, 977. (e) DeArmond, M. K.; Hanck, K. W.; Wertz, D. W. *Coord. Chem. Rev.* **1985**, *64*, 65. (f) Ohsawa, Y.; DeArmond, M. K.; Hanck, K. W.; Moreland, C. G. *J. Am. Chem. Soc.* **1985**, *107*, 5383. (g) Tait, C. T.; MacQueen, D. B.; Donohoe, R. J.; DeArmond, M. K.; Hanck, K. W.; Wertz, D. W. *J. Phys. Chem.* **1986**, *90*, 1766. (h) Gex, J. N.; DeArmond, M. K.; Hanck, K. W. *Ibid.* **1987**, *91*, 251. (i) Gex, J. N.; Cooper, J. B.; Hanck, K. W.; DeArmond, M. K. *Ibid.* **1987**, *91*, 4686. (j) Gex, J. N.; Brewer, W.; Bergmann, K.; Tait, C. D.; DeArmond, M. K.; Hanck, K. W.; Wertz, D. W. *Ibid.* **1987**, *91*, 4776. (k) Tait, C. D.; Vess, T. M.; DeArmond, M. K.; Hanck, K. W.; Wertz, D. W. *J. Chem. Soc., Dalton Trans.* **1987**, 2467. (l) Gex, J. N.; DeArmond, M. K.; Hanck, K. W. *Inorg. Chem.* **1987**, *26*, 3236. (m) Berger, R. M.; McMillin, D. R. *Ibid.* **1988**, *27*, 4245.

(4) (a) Braterman, P. S.; Heath, G. A.; Yellowlees, L. J. *J. Chem. Soc., Dalton Trans.* **1981**, 1801. (b) Kober, E. M.; Meyer, T. J. *Inorg. Chem.* **1982**, *21*, 3967. (c) *Ibid.* **1984**, *23*, 3877. (d) Braterman, P. S. *Ibid.* **1986**, *25*, 1732. (e) Yersin, H.; Gallhuber, E.; Hensler, G. *Chem. Phys. Lett.* **1987**, *134*, 497. (f) Ferguson, J.; Krausz, E. *Inorg. Chem.* **1987**, *26*, 1383. (g) Myrick, M. L.; Blakley, R. L.; DeArmond, M. K.; Arthur, M. L. *J. Am. Chem. Soc.* **1988**, *110*, 1325.

(5) (a) Krause, R. A. *Struct. Bonding Berlin* **1987**, *67*, 1. (b) Juris, A.; Balzani, V.; Barigelletti, F.; Campagna, S.; Belser, P.; von Zelewsky, A. *Coord. Chem. Rev.* **1988**, *84*, 85.

(6) Ernst, S. D.; Kaim, W. *Inorg. Chem.* **1989**, *28*, 1520.

(7) (a) Kaim, W. *Coord. Chem. Rev.* **1987**, *76*, 187. (b) von Zelewsky, A.; Daul, C.; Schläpfer, C. W. *Landolt-Börnstein, Physical and Chemical Tables*; Springer-Verlag: West Berlin, 1987; New Series, Vol. II/17a, p 199.

(8) (a) Rillema, D. P.; Allen, G.; Meyer, T. J.; Conrad, D. *Inorg. Chem.* **1983**, *22*, 1617. (b) Barigelletti, F.; Juris, A.; Balzani, V.; Belser, P.; von Zelewsky, A. *Ibid.* **1987**, *26*, 4115. (c) Tazuke, S.; Kitamura, N. *Pure Appl. Chem.* **1984**, *56*, 1269.

0002-7863/90/1512-173$02.50/0